ISSN 1674-1056
http://cpb.iphy.ac.cn
http://iopscience.iop.org/cpb
中国物理 B
Chinese Physics
中国物理
Chinese Physics B

Dependence of switching process on the perpendicular magnetic anisotropy constant in P-MTJ

Mao-Sen Yang(杨茂森), Liang Fang(方粮), Ya-Qing Chi(池雅庆)

Citation: Chin. Phys. B . 2018, 27(9): 098504. **doi:** 10.1088/1674-1056/27/9/098504

Journal homepage: http://cpb.iphy.ac.cn; http://iopscience.iop.org/cpb

What follows is a list of articles you may be interested in

Real-space observation of individual skyrmions in helimagnetic nanostripes

Jin Chi-Ming, Du Hai-Feng

Chin. Phys. B . 2015, 24(12): 128501. **doi:** 10.1088/1674-1056/24/12/128501

Low frequency noise in asymmetric double barrier magnetic tunnel junctions with a top thin MgO layer

Guo Hui-Qiang, Tang Wei-Yue, Liu Liang, Wei Jian, Li Da-Lai, Feng Jia-Feng, Han Xiu-Feng

Chin. Phys. B . 2015, 24(7): 078504. **doi:** 10.1088/1674-1056/24/7/078504

Investigation of $L1_0$ FePt-based soft/hard composite bit-patterned media by micromagnetic simulation

Wang Ying, Wei Dan, Cao Jiang-Wei, Wei Fu-Lin

Chin. Phys. B . 2015, 24(6): 068504. **doi:** 10.1088/1674-1056/24/6/068504

Recent progress in perpendicularly magnetized Mn-based binary alloy films

Zhu Li-Jun, Nie Shuai-Hua, Zhao Jian-Hua

Chin. Phys. B . 2013, 22(11): 118505. **doi:** 10.1088/1674-1056/22/11/118505

Micromagnetic simulation with three models of FeCo/$L1_0$ FePt exchange-coupled particles for bit-patterned media

Wang Ying, Wang Rui, Xie Hai-Long, Bai Jian-Min, Wei Fu-Lin

Chin. Phys. B . 2013, 22(6): 068506. **doi:** 10.1088/1674-1056/22/6/068506

Dependence of switching process on the perpendicular magnetic anisotropy constant in P-MTJ*

Mao-Sen Yang(杨茂森)[1], Liang Fang(方粮)[1,†], and Ya-Qing Chi(池雅庆)[2]

[1] State Key Laboratory of High-Performance Computing, College of Computer, National University of Defense Technology, Changsha 410073, China
[2] Institute of Microelectronics, College of Computer, National University of Defense Technology, Changsha 410073, China

(Received 1 May 2018; revised manuscript received 7 June 2018; published online 10 August 2018)

We investigate the dependence of the switching process on the perpendicular magnetic anisotropy (PMA) constant in perpendicular spin transfer torque magnetic tunnel junctions (P-MTJs) using micromagnetic simulations. It is found that the final stable states of the magnetization distribution of the free layer after switching can be divided into three different states based on different PMA constants: vortex, uniform, and steady. Different magnetic states can be attributed to a trade-off among demagnetization, exchange, and PMA energies. The generation of the vortex state is also related to the non-uniform stray field from the polarizer, and the final stable magnetization is sensitive to the PMA constant. The vortex and uniform states have different switching processes, and the switching time of the vortex state is longer than that of the uniform state due to hindrance by the vortex.

Keywords: magnetic tunnel junction, perpendicular magnetic anisotropy, vortex state, micromagnetic simulation

PACS: 85.75.Dd, 85.70.Ay, 75.78.Cd, 74.25.Ha **DOI:** 10.1088/1674-1056/27/9/098504

1. Introduction

The STT-MRAM has attracted extensive attention from academia and industry as a novel nonvolatile memory technology since 1996.[1,2] Due to its fast programming speed, high storage density, and low energy consumption, STT-MRAM has become one of the strongest contenders among nonvolatile memory candidates.[3–6] Compared with the traditional in-plane STT-MRAM, perpendicular STT-MRAM,[7–10] with its unique theoretical advantages of lower switching current density and higher thermal stability, has become the mainstream type of STT-MRAM. It is common knowledge that switching current density is very sensitive to the spin configuration and dynamics of magnetic tunnel junctions (MTJs). However, with the further reduction in device dimension, the junction dimension is comparable to the exchange length of the system,[11] which makes spin configurations very susceptible to fabrication processes,[12–14] and the current density becomes less predictable. Therefore, stabilization and manipulation of the spin configurations become key problems that need to be solved urgently. To overcome these problems, the study of the underlying physics of the switching mechanisms of perpendicular MTJs (P-MTJ) is essential. It is well known that the perpendicular magnetic anisotropy (PMA)[7,15] constant, K_u, plays an important role in the switching process of P-MTJs. Many studies focus on the dependence of PMA on magnetic multilayer film structures, such as CoFeB/Pt and CoFeB/Ni,[16,17] but the detailed mechanism by which K_u affects the switching process is still not clear. Because most investigations of the switching process have been based on the macrospin model,[18,19] such a mechanism cannot be explained with a simple macrospin model. Only micromagnetic simulations can reveal the detailed spin dynamics during the switching process. Therefore, micromagnetic simulations are essential to obtain deep insights into the switching processes.

In this study, we systematically investigated the switching process dependence on K_u for typical P-MTJ structures with a wide range of K_u by employing the Object Oriented Micromagnetic Framework (OOMMF),[20] a public domain simulator, with the public STT extension module.[21] We calculated the average normalized out-of-plane magnetization M_z/M_s and found the final stable spin configurations of the free layer with various K_u. According to these results, the final stable state of the free layer can be divided into three different states: vortex, uniform, and steady. In addition, we analyzed the formation mechanism of the three different states, especially for the vortex state and its correlation with K_u. Finally, through showing the time evolution of the spin configurations, the effects of K_u on the vortex and uniform state switching processes are compared.

2. Micromagnetic simulations

Figure 1 shows the typical P-MTJ structures. The thicknesses of the F_{Free}, Insulator, and $F_{Polarizer}$ layers were 2, 1, and 1 nm, respectively. The saturation magnetizations of F_{Free} and $F_{Polarizer}$ were 1.3×10^6 A/m. The interface PMA energy, K_s, of the free layer was varied from 0.5×10^{-4}

*Project supported by the National Natural Science Foundation of China (Grant No. 61332003) and the Natural Science Foundation of Hunan Province, China (Grant No. 2015JJ3024).

†Corresponding author. E-mail: lfang@nudt.edu.cn

© 2018 Chinese Physical Society and IOP Publishing Ltd

to 1.0×10^{-3} J/m^2. In the micromagnetic simulations, we set the perpendicular volume anisotropy K_u with the relation $K_u = K_s/t_{Free}$ to implement the interface anisotropy.[7] A bias field of 4×10^5 A/m was assigned to the negative z-direction to pin the magnetization of the $F_{Polarizer}$ layer. The shapes of the MTJs were fixed as 40 nm diameter circular disks, as shown in Fig. 1. The exchange stiffness constant $A_{ex} = 3.0 \times 10^{11}$ J/m and the Gilbert damping constant $\alpha = 0.02$ were fixed in the present work. The unit cell size was $1 \times 1 \times 1$ nm^3. The initial magnetization distribution state was set as uniform. Positive current was defined as flowing from the polarizer to the free layers. The positive current prefered antiparallel (AP) configurations, as shown in Fig. 1. We applied a specific current density of $J_c = 2.0 \times 10^{11}$ A/m^2 for 10 ns from the initial uniform spin configuration to ensure that the magnetization can be switched completely and then waited for 2 ns more with zero current to relax the spin magnetic moment. After the 12 ns simulation time, we checked the magnetization configuration and determined the switching status. More details of the micromagnetic simulations can be found in the previous report.[21,22] For simplicity, we ignored the field-like term, and all simulations were performed at 0 K. Thermal activation spin motion was not considered.

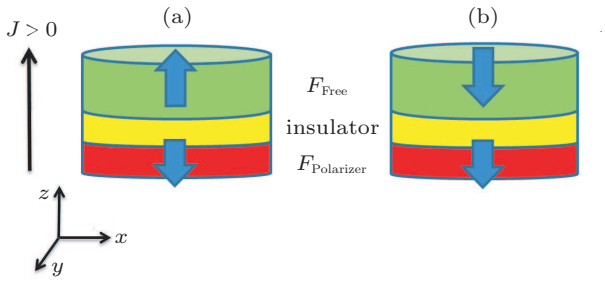


Fig. 1. (color online) Typical perpendicular magnetic tunnel junction (P-MTJ) structure of (a) anti-parallel state of MTJ, and (b) parallel state of MTJ. F_{Free} and $F_{Polarizer}$ are the ferromagnetic free layer and fixed layer; the insulator layer is sandwiched between F_{Free} and $F_{Polarizer}$. The current direction and coordinate system are as shown.

3. Results and discussion

We calculated the average normalized out-of-plane magnetization, M_z/M_s, of the free layers of AP-parallel (P) and P-AP switching processes with various K_u. To implement the interface anisotropy, we varied K_u from 1.0×10^5 to 2.0×10^6 J/m^3 because the surface PMA of the free layers were varied from 0.5×10^{-4} to 1.0×10^{-3} J/m^2. Figure 2 shows the results of M_z/M_s of the P-AP and AP–P switching processes for various K_u for the P-MTJ structure. The final state can be divided into three types based on K_u: vortex, uniform, and stable states. The vortex state is found for $K_u < 0.7 \times 10^6$ J/m^3. In this regime, the magnetization direction is not fully reversed; the final magnetization distribution of the free layer shows a vortex state, as shown in the inset map. Similar to the vortex for the in-plane anisotropy materials, the PMA vortex has a vortex core where the magnetization direction is perpendicular to the plane, and the other parts of the vortex are in-plane magnetized with a chiral structure. In addition, the average normalized out-of-plane magnetization increased with increasing K_u. The uniform state was obtained for 0.7×10^6 J/m^3 $< K_u < 1.3 \times 10^6$ J/m^3. As shown in the inset map, the magnetization direction was completely reversed, and this was the normal work area. When $K_u > 1.4 \times 10^6$ J/m^3, no change occurred in the magnetization direction for the free layer, which remained in the initial state. The variation tendencies of the magnetization for the final stable state with the increase of K_u for the initially AP and P states are almost symmetric, but the absolute value of magnetization for the initially AP state is larger than that of P owing to the opposing characteristics of the stray field from the polarizer.

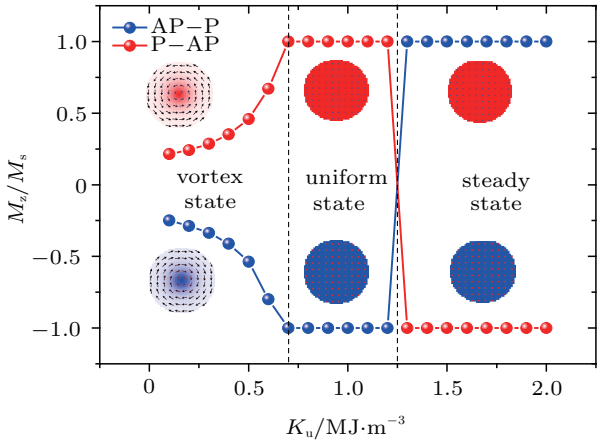


Fig. 2. (color online) Stable average normalized out-of-plane magnetizations, M_z/M_s, with various perpendicular magnetic anisotropy (PMA) constants, K_u, for the free layer stable state after switching, initially parallel (P)-states (red curve) and initially antiparallel (AP)-states (blue curve). Three different regimes are indicated and separated by vertical dashed lines. Insets: examples of spatial distribution of the magnetization related to each region. The colors refer to the z component of the magnetization (red positive, blue negative).

Considering that the stable state of spin configuration is determined by the trade-off of inner energy,[23] the stable state of the free layer after switching for the initial P-state is the same as that after relaxation for the initial AP-state. Thus, we can explain the mechanism of vortex generation by analyzing the relaxation process for the corresponding initial state. Although there have been many previous studies on vortex states,[24–27] all of the research was focused on the in-plane magnetic anisotropy (IMA) materials. As a result, the detailed mechanism of vortex generation and the correlation with K_u for PMA materials still need to be elaborated.[28] Figure 3 shows the relaxation process for the initial AP-state with $K_u = 0.2 \times 10^6$ J/m^3. When $K_u < 0.7 \times 10^6$ J/m^3, the maximum PMA energy is smaller than the initial demagnetization energy; therefore, the initial uniform distribution of magnetization is unstable and will precess to the in-plane direction. Owing to the non-uniform stray field from the polarizer layer and the finite size edge effect, the spins at the edge easily de-

viate from the positive z-axis. Then, under the influence of exchange interactions, the adjacent internal magnetic moments are driven to precess, and they propagate from the edge to the center, finally producing a vortex core at the center, as shown in Fig. 3(d).

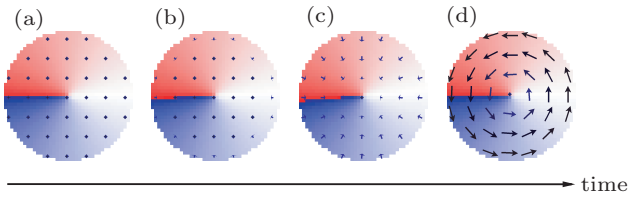


Fig. 3. (color online) Example of snapshots for the relaxation process of free layer with perpendicular magnetic anisotropy (PMA) constant $K_u = 0.2 \times 10^6$ J/m^3, initially anti-parallel (AP)-states. (a) Initial state: uniform out-of-plane. (b) The spins at the edge have a deviation from the $+z$-axis. (c) Initial uniform area shrinks gradually. (d) Vortex state formation.

When $K_u > 0.7 \times 10^6$ J/m^3, the maximum PMA energy is greater than the initial demagnetization energy; therefore, the final magnetization distribution after switching maintains a uniform state that is perpendicular to the horizontal plane. It is common knowledge that the intrinsic threshold current is proportional to K_u for the P-MTJ.[7] When the value of K_u increases to 1.3×10^6 J/m^3, the current density $J_c = 2.0 \times 10^{11}$ A/m^2 that was set in our simulation is not enough to overcome the anisotropy energy, and the magnetization of the free layer thus remains in the initial state.

To analyze the dependence of the vortex state on K_u in depth, we plot the total, exchange, demagnetization, and PMA energies as functions of K_u for the free layer stable state after switching for initially AP-states in Fig. 4. When $K_u > 0.7 \times 10^6$ J/m^3, the total and demagnetization energies reach their peak values and do not change further, and the exchange and PMA energies are both zero. When $K_u < 0.7 \times 10^6$ J/m^3, the total and demagnetization energies decrease with the decrease of K_u. Considering that the relationship between the demagnetization energy and average out-of-plane magnetizations can be expressed simply as $E_{Dem} = 1/2\mu_0 M_z^2$, the stable average normalized out-of-plane magnetizations, M_z/M_s, of the vortex state also decrease with decreasing K_u. The exchange energy increases with decreasing K_u, which hinders the decrease of the demagnetization energy. Thus, the decline rate of the average normalized out-of-plane magnetizations for the vortex state gradually decreases, as shown in Fig. 2. The relationship between the PMA energy and angle of magnetization from positive z-axis can be expressed simply as $E_{PMA} = K_u \sin^2\theta$. Thus, the PMA energy will have a nonmonotonic relationship with K_u, and the value of the PMA energy reaches a peak at $K_u = 0.5 \times 10^6$ J/m^3, as shown in Fig. 4.

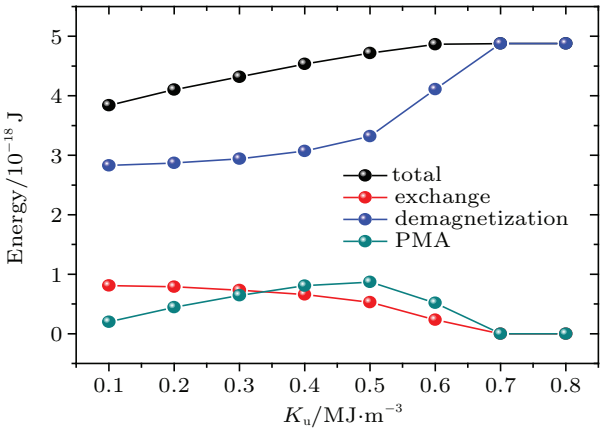


Fig. 4. (color online) Total, exchange, demagnetization, and perpendicular magnetic anisotropy (PMA) energies as a function of the PMA constant, K_u, for the stable state of free layer after switching for initially antiparallel (AP)-states.

Finally, to show the switching process of different states more intuitively, we obtained snapshots of the spin configurations of the free layer for the AP–P switching process at $K_u = 0.2 \times 10^6$ J/m^3 and $K_u = 0.7 \times 10^6$ J/m^3, as shown in Figs. 5 and 6, respectively. As shown in Fig. 5, the switching process can be divided into three sub-processes in the time dimension: nucleation, periodic precession, and damping oscillation. Nucleation is the formation of the vortex state; it is different from relaxation in that the effect of the polarization current accelerates the formation of the vortex state. During periodic precession, the spin configuration changes periodically in the order of counter-clockwise, inward radial, clockwise, and outward radial vortex directions.[29] When the central vortex nucleus flips over, the spin configuration enters the damping oscillation process, and the chirality of the vortex state remains in the counter-clockwise direction. Each magnetic moment is damped to the stable state around its equilibrium position, as shown in Fig. 7. The position of the final stable state is determined by the energy trade-off of the system, as discussed earlier.

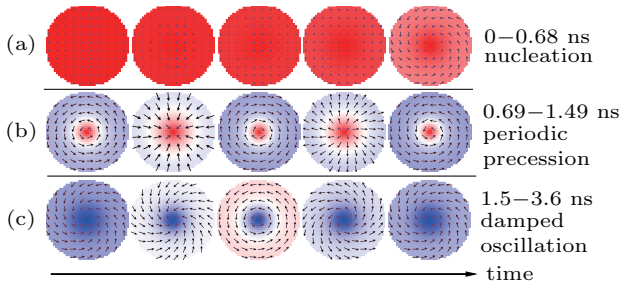


Fig. 5. (color online) Time evolution of spin configurations of the free layer for AP–P switching process at $K_u = 0.2 \times 10^6$ J/m^3. (a) Nucleation, (b) periodic precession, and (c) damped oscillation.

Figure 6 shows the switching process of the uniform state. The first two sub-processes are the same as those of the vortex state, but the last process is replaced by spin-wave emission,[25] as shown in Fig. 7. In the spin-wave emission

process, the uniform distribution of the magnetic moments begins from the center area and propagates to the edge in the form of waves. The waves will then be reflected after reaching a certain distance, but the area of the uniform distribution state after reflection is larger than that of the initial state. In this way, all the magnetic moments are finally in a uniform state, as shown in Fig. 6(c). Comparing the two different switching processes, it is not difficult to observe that the switching time of the vortex state is much longer than that of the uniform state, although the PMA constant of the vortex state is smaller than that of the uniform state. This is mainly attributed to the last damped oscillation time, which is about 2.1 ns, whereas the spin-wave emission time is only 0.3 ns. Thus, we can conclude that the generation of the vortex state hinders the reversal of magnetization.

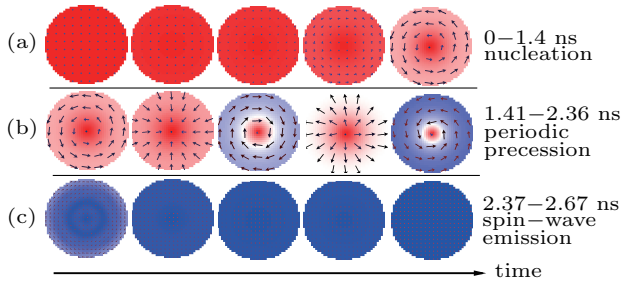


Fig. 6. (color online) Time evolution of spin configurations of the free layer for AP–P switching process at $K_u = 0.7 \times 10^6$ J/m^3. (a) Nucleation, (b) periodic precession, and (c) spin-wave emission.

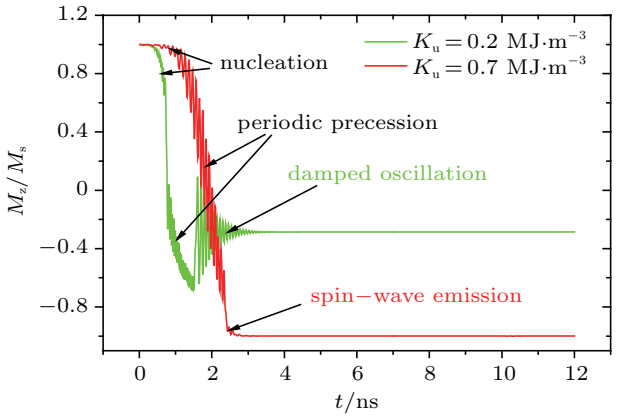


Fig. 7. (color online) Time-dependent average normalized out-of-plane magnetizations M_z/M_s for the initially AP-states MTJ structure with various K_u (0.2, 0.7 MJ/m^3).

4. Conclusions

The final stable states of the spin configurations after current induced switching for P-MTJ are divided into three types as vortex, uniform and steady states based on the value of the PMA constant. The mechanism can be explained by the energy trade-off in the system. The generation of the vortex state is attributed to the non-uniform stray field from the polarizer, and the variations of the demagnetization, exchange, and PMA energies determine the final stable state. Besides, the average out-of-plane magnetization component of the vortex state is sensitive to the PMA constant. Finally, we demonstrate the time evolution of the spin configurations for the switching processes of the vortex and uniform states and find that the switching time of the vortex state is longer than that of the uniform state because of the hindering action of the vortices in the switching process. Therefore, avoiding the vortex state may be an effective way to improve the switching speed of the P-MTJ.

References

[1] Slonczewski J C 1996 *J. Magn. Magn. Mater.* **159** L1-L7
[2] Berger L 1996 *Phys. Rev. B* **54** 9353
[3] Kawahara T, Ito K, Takemura R and Ohno H 2012 *Microelectron. Reliab.* **52** 613
[4] Tang Z, Fang L, Xu N and Liu R 2015 *J. Appl. Phys.* **118** 185309
[5] Hosomi M, Yamagishi H, Yamamoto T, Bessho K, Higo Y, Yamane K, Yamada H, Shoji M, Hachino H, Fukumoto C, Nagao H and Kano H 2005 *Proceedings of the IEEE International Electron Devices Meeting*, December 5-5, 2005, Washington DC, USA, pp. 459–462
[6] Tang Z, Chi Y, Fang L, Liu R and Yi X 2014 *J. Nanosci. Nanotech.* **14** 1494
[7] Ikeda S, Miura K, Yamamoto H, Mizunuma K, Gan H D, Endo M, Kanai S, Hayakawa J, Matsukura F and Ohno H 2010 *Nat. Mater.* **9** 721
[8] Mangin S, Ravelosona D, Katine J A, Carey M J, Terris B D and Fullerton E E 2006 *Nat. Mater.* **5** 210
[9] Nakayama M, Kai T, Shimomura N, Amano M, Kitagawa E, Nagase T, Yoshikawa M, Kishi T, Ikegawa S and Yoda H 2008 *J. Appl. Phys.* **103** 07A710
[10] Ikeda S, Hayakawa J, Lee Y M, Matsukura F, Ohno Y, Hanyu T and Ohno H 2007 *IEEE Trans. Electron Dev.* **54** 991
[11] You C Y and Jung M 2013 *J. Appl. Phys.* **113** 073904
[12] Sun J Z, Trouilloud P L, Gajek M J, Nowak J, Robertazzi R P, Hu G, Abraham D W, Gaidis M C, Brown S L, O'Sullivan E J, Gallagher W J and Worledge D C 2012 *J. Appl. Phys.* **111** 07C711
[13] Sun J Z, Robertazzi R P, Nowak J, Trouilloud P L, Hu G, Abraham D W, Gaidis M C, Brown S L, O'Sullivan E J, Gallagher W J and Worledge D C 2011 *Phys. Rev. B* **84** 064413
[14] Chenchen J W, Akhtar M A K B, Sbiaa R, Hao M, Sunny L Y H, Kai W S, Ping L, Carlberg P and Arthur A K S 2012 *Jap. J. Appl. Phys.* **51** 013101
[15] Liu Y, Zhu K G, Zhong H C, Zhu Z Y, Yu T and Ma S D 2016 *Chin. Phys. B* **25** 117805
[16] Liu N, Wang H and Zhu T 2012 *Acta Phys. Sin.* **61** 167504
[17] Ju H L, Wang H X, Cheng P, Li B H, Chen X B, Liu S Y and Yu G H 2016 *Acta Phys. Sin* **65** 247502
[18] Zhang Y, Zhao W S, Lakys Y, Klein J O, Kim J V, Ravelosona D and Chappter C 2012 *IEEE Trans. Electron Dev.* **59** 819
[19] Panagopoulos G, Augustine C and Roy K 2012 *Proceedings of the IEEE Design, Automation & Test in Europe Conference & Exhibition*, March 12-16, 2012, Dresden, Germany, pp. 1443-1446
[20] Donahue M J and Porter D G: OOMMF User's Guide,Ver. 1.0, *Interagency Report NISTIR* 6376, NIST, USA(1999).
[21] You C Y 2012 *J. Magn.* **17** 73
[22] You C Y 2014 *J. Appl. Phys.* **115** 043914
[23] You C Y 2013 *J. Magn.* **18** 380
[24] Kim J S, Kläui M, Fistul M V, Yoon J, You C Y, Mattheis R, Ulysse C and Faini G 2013 *Phys. Rev. B* **88** 064402
[25] Kim J S, Boulle O, Verstoep S, Heyne L, Rhensius J, Kläui M, Heyderman L J, Kronast F, Mattheis R, Ulysse C and Faini G 2010 *Phys. Rev. B* **82** 104427
[26] Kasai S, Nakatani Y, Kobayashi K, Kohno H and Ono T 2006 *Phys. Rev. Lett.* **97** 107204
[27] Kim J Y and Choe S B 2007 *J. Magn.* **12** 113
[28] Su Y C, Lei H Y and Hu J G 2015 *Chin. Phys. B* **24** 097506
[29] Siracusano G, Tomasello R, Giordano A, Puliafito V, Azzerboni B, Ozatay O, Carpentieri M and Finocchio G 2016 *Phys. Rev. Lett.* **117** 087204